Pipeline for automatic segmentation of multiparametric MRI data in a rat model of ischemic stroke

Duoyao Liang, Marlène Wiart, Fabien Chauveau, Thomas Grenier

▶ **To cite this version:**

Duoyao Liang, Marlène Wiart, Fabien Chauveau, Thomas Grenier. Pipeline for automatic segmentation of multiparametric MRI data in a rat model of ischemic stroke. SPIE Medical Imaging - Clinical and Biomedical Imaging, SPIE, pp.26, 2024, 10.1117/12.3006149 . hal-04798846

HAL Id: hal-04798846
https://hal.science/hal-04798846v1

Submitted on 22 Nov 2024

HAL is a multi-disciplinary open access archive for the deposit and dissemination of scientific research documents, whether they are published or not. The documents may come from teaching and research institutions in France or abroad, or from public or private research centers.

L'archive ouverte pluridisciplinaire **HAL**, est destinée au dépôt et à la diffusion de documents scientifiques de niveau recherche, publiés ou non, émanant des établissements d'enseignement et de recherche français ou étrangers, des laboratoires publics ou privés.

Please verify that (1) all pages are present, (2) all figures are correct, (3) all fonts and special characters are correct, and (4) all text and figures fit within the red margin lines shown on this review document. Complete formatting information is available at http://SPIE.org/manuscripts

Return to the Manage Active Submissions page at http://spie.org/submissions/tasks.aspx and approve or disapprove this submission. Your manuscript will not be published without this approval. Please contact authorhelp@spie.org with any questions or concerns.

Pipeline for automatic segmentation of multiparametric MRI data in a rat model of ischemic stroke

Duoyao LIANG[a], Marlène WIART[a], Fabien CHAUVEAU[b], and Thomas GRENIER[c]

[a]CarMeN, Inserm U1060, INRAE U1379, INSA Lyon, Univ Claude Bernard Lyon 1, France
[b]CRNL, Inserm U1028, CNRS UMR5292, France
[c]Univ Lyon, INSA-Lyon, Université Claude Bernard Lyon 1, UJM-Saint Etienne, CNRS, Inserm, CREATIS UMR 5220, U1294, Lyon, France

ABSTRACT

Stroke is a global health concern, positioning itself as one of the chief culprits behind both disability and mortality worldwide. There is currently no treatment for ischemic stroke besides reperfusion therapy. To evaluate new treatment options, researchers conduct studies on rat models of ischemic stroke using the same MRI approach as in patients. MR images and parametric maps are used to define the ischemic core, the area-at-risk of infarction and the final lesion.

Historically, this process has relied heavily on manual segmentation conducted by experts, which not only consumes a significant amount of time but also often lacks the desired level of reliability. This drawback establishes an urgent requirement for robust, dependable, and automated tools to stimulate progress in stroke research.

Addressing this pressing need, we introduce a novel pipeline that automates lesion segmentation in a rat stroke model of ischemic stroke. This innovative solution ingeniously amalgamates steps of pre-processing, optimal thresholding, and the state-of-the-art UNet deep learning method. From our knowledge, we are the first to propose an automatic segmentation of regions from T2, DWI and PWI MRI imaging.

The integrated approach of optimal thresholding and UNet employed in this pipeline delivers high-quality results. We evaluated the processing performance on 58 rats using 4 measures of segmentation quality and also correlation curves between lesion size and manual versus automatic segmentation. With this robust tool, the segmentation of abnormalities in rat model is made both efficient and precise, saving valuable time and resources. Therefore, our results hold the potential to propel advancements in stroke research and stimulate the development of pioneering treatment strategies.

Our code and data (with manual annotations) are available online.

Keywords: Stroke, pre-clinical research, multi-parametric MRI, segmentation, deep learning

1. INTRODUCTION

Ischemic stroke is a major public health issue. Today, there is no treatment option for patients with ischemic stroke besides reperfusion therapy. However, even in case of successful re-perfusion, half of the patients suffer from long-term neurological disabilities. There is therefore an urgent need for the discovery of novel treatments that would alleviate the handicap burden in this condition. In this context, pre-clinical research in rodent models of ischemic stroke is needed to evaluate and select drugs and therapeutic strategies that may improve stroke outcome.[1]

Imaging is pivotal in diagnosing ischemic stroke and defining patients' eligibility for reperfusion therapy. Multiparametric MRI is the method of choice to achieve this aim.[2] The "ischemic penumbra" is defined as the mismatch between perfusion and diffusion lesion during the arterial occlusion. It is used as a proxy of the viable tissue that may be salvaged by therapy. In the interest of clinical translation, we systematically perform multi-parametric MRI during the arterial occlusion in our rat model of ischemic stroke.[3] However, manual

Further author information: (Send correspondence to Thomas Grenier - E-mail: thomas.grenier@creatis.insa-lyon.fr)

SPIE USE: ____ DB Check, ____ Prod Check, Notes:

Please verify that (1) all pages are present, (2) all figures are correct, (3) all fonts and special characters are correct, and (4) all text and figures fit within the red margin lines shown on this review document. Complete formatting information is available at http://SPIE.org/manuscripts

Return to the Manage Active Submissions page at http://spie.org/submissions/tasks.aspx and approve or disapprove this submission. Your manuscript will not be published without this approval. Please contact authorhelp@spie.org with any questions or concerns.

delineation of perfusion maps, apparent diffusion maps (to define the ischemic penumbra), and follow-up T2-weighted imaging (to define tissue outcome) is time-consuming and user-dependent. There is therefore a need for developing automatic tools that will register and segment the maps and images of interest to assist image analysis.

According to a literature review, deep learning appears well suited for a large panel of challenging medical image analysis problems and incorporates pre- and post-processing:..[4–8] For medical image segmentation, the central network architecture is UNet. It was proposed in[9] and was improved many times.[10–12] Recent advances in transformers[13] and foundation models[14] can be interesting alternatives to classical UNet, but they require a very large set of annotated images and huge computing GPU resources. For our automatic segmentation of MRI maps, we optimize a threshold and train two classic UNet. We also have taken care of the pre-processing and data augmentation required to train the networks.

In the following, we first present the rat MRI dataset and the parametric maps used. Then, we detail the proposed automatic processing pipeline that allows segmentation. We end with a results section and discussion.

2. DATASET

We used a dataset of 58 rats with transient middle cerebral artery occlusion (tMCAO, 90 minutes) that underwent MRI during the occlusion (H0: perfusion-weighted imaging PWI, diffusion-weighted imaging DWI and T2-weighted imaging or T2H0) and a follow-up MRI the day after (H24: T2-weighted imaging or T2H24). MR images were acquired on a 7T Bruker MRI magnet interfaced with Paravision 5.0. For all sequences, the field of view was $35 \times 35mm$, slice thickness was $1mm$ and 15 slices were acquired.

PWI was obtained with dynamic contrast-enhanced MRI (DSC-MRI) before, during and after an intravenous bolus injection of Gd-DOTA (DOTAREM, Guerbet, France) at $0.6ml/kg$, using the following parameters: TE/TR: $8.2/600ms$, flip angle: 50°, matrix 80×80, 100 repetitions (duration: 1 minute).

DWI was obtained with echo planar imaging (EPI), using the following parameters: TE/TR: $23.2/5000ms$, b value: 0, 1500, 3000 s/mm2, flip angle: 90°, matrix: 128×128 (duration: 4 minutes 40 seconds).

T2-weighted imaging was obtained with 2D RARE sequence (RARE factor of 8), using the following parameters: TE/TR: $75/5000ms$, flip angle: 180°, matrix: 256×256 (duration: 4 minutes 44 seconds).

Parametric maps were computed to generate maximum peak concentration (MPC) maps from PWI (defined as the peak of the deltaR2*-time curve for each voxel) and apparent diffusion coefficient (ADC) maps from DWI. The lesion on DWI represents the ischemic core. The PWI-DWI mismatch defines the ischemic penumbra, which is the tissue that may be salvaged by treatment. Following the work of Debatisse *et al.*,[2] we defined 4 regions with different fate at H24: infarcted core, salvaged core, infarcted penumbra, salvaged penumbra.

The dataset comprises 58 masked rats and 10 no-masked rats with a transient middle cerebral artery occlusion (tMCAO, 90 minutes) and longitudinal MRI (per-occlusion MRI at H0 and follow-up MRI at H24). For each rat, four sequences are used to carry out this research: T2H0, DWI H0, PWI H0, and T2H24. Each sequence has 15 slices in the rat brain. An expert have manually segmented the lesions in the following sequences: DWI, PWI and T2H24 in the original space. The images and their manual segmentations are available online*.

3. METHODS

The complete procedures of the 4 operational regions' segmentation pipeline are outlined in figure 1. The code of the pipeline is available on github†. Four MRI sequences are used as input: three at H0 (T2H0, PWI, and DWI), and one 24 hours later (T2H24). The remaining of this section explains the dedicated process applied to these sequences.

*https://www.creatis.insa-lyon.fr/~grenier/?p=1317 with "SPIE" password
†https://github.com/L221y/RatStrokeSegmentation

SPIE USE: ____ DB Check, ____ Prod Check, Notes:

Please verify that (1) all pages are present, (2) all figures are correct, (3) all fonts and special characters are correct, and (4) all text and figures fit within the red margin lines shown on this review document. Complete formatting information is available at http://SPIE.org/manuscripts

Return to the Manage Active Submissions page at http://spie.org/submissions/tasks.aspx and approve or disapprove this submission. Your manuscript will not be published without this approval. Please contact authorhelp@spie.org with any questions or concerns.

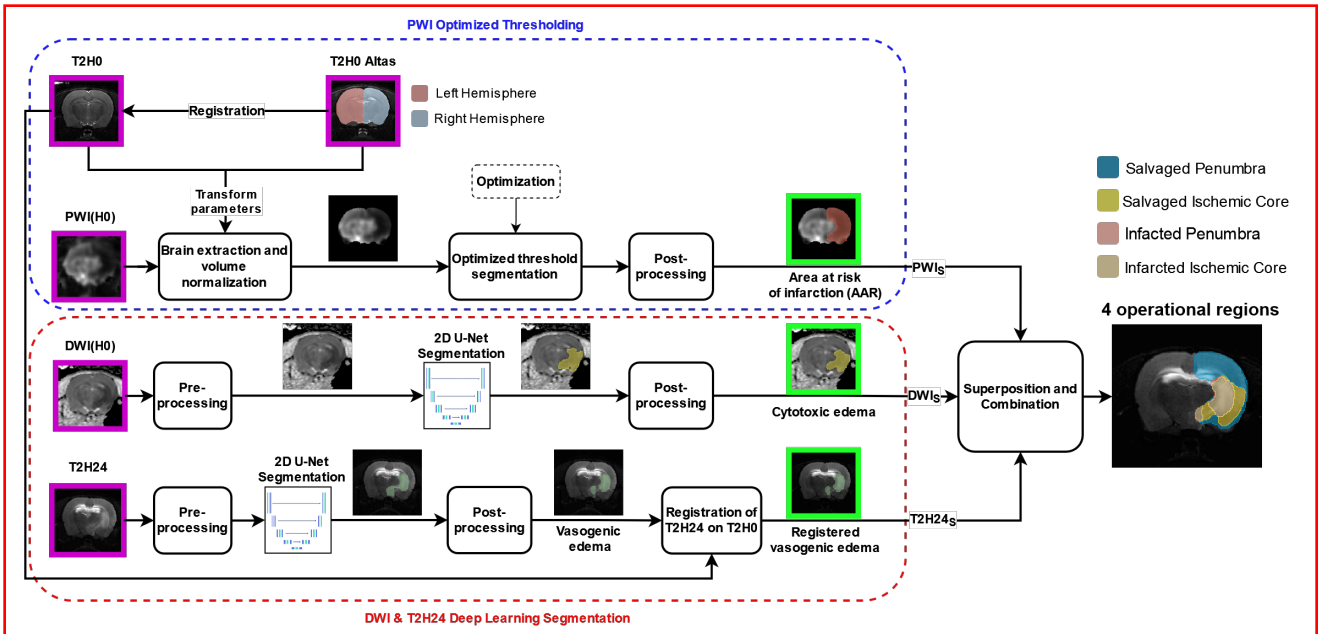

Figure 1: Proposed pipeline segmentation approach to obtain the 4 regions of interest. MRI inputs T2H0, T2H24, PWI(H0) and DWI(H0) are highlighted in purple, and obtained segmentations are highlighted in green.

3.1 PWI Optimized Threshold Segmentation

In 2, authors suggest using a simple threshold on PWI volumes to extract the Area At Risk of Infarction (AAR) as in clinical usage. We adapt this approach to our dataset of rats and compute an optimized threshold.

This task starts by extracting the brain and identifying each hemisphere of the PWI image using coregistered T2H0 volumes. We first register a manually T2H0 atlas volume, with its brain and hemisphere masks, to all the other T2H0 rats' volumes using a rigid transform and an affine transform[15] using Elastix.[16,17] Since the DWI, PWI, and T2H0 are acquired during the same exam, the DWI and PWI brains and the contralateral hemisphere of all rats are extracted by propagating the masks registered on T2H0. The brain PWI volume intensities are then normalized to a percentage by dividing each intensity of the brain by the median intensity value of the contralateral hemisphere extracted during the previous step.

We then determine the threshold values that maximize the Sørensen–Dice coefficient of each 20 PWI manual mask used as ground truth. The average of these threshold values, 75%, is then used for all PWI volumes to obtain the AAR masks. As usual, post-processing is needed to clean such obtained masks. The following operations are applied sequentially: a median filter of size $[3, 3, 1]$, a morphological closing filter of size $[9, 9, 1]$, and a morphological opening filter of size $[5, 5, 1]$. Subsequently, all contralateral regions are removed, and only the largest connected component is retained. This mask, noted PWI_S, is the AAR region for our rats.

3.2 T2H24 and DWI Deep Learning Segmentations

To conduct the segmentation of DWI and T2H24 using deep learning networks, the 2D UNet[9] architecture is chosen due to its robustness, simplicity, and efficiency according to our dataset. We use Monai[18] to conduct this network. For both T2H24 and DWI images, pre- and post-processings are the same but segmentation is performed using two different training of the same 2D-UNet, one for each sequence.

The pre-processing stage involves two key steps: volume cropping and standardization. To eliminate information outside the brain, the entire volume is cropped from its original size of 256×256 to 150×150. Subsequently, the volume intensities are standardized, to a mean value of 0, and a standard deviation of 1.

Then, during inference, the preprocessed volumes are fed slice by slice as input to the 2D UNet network. All slices are segmented individually and then 3D volumes are reconstructed to the same size and resolution as the input volumes. However, networks need to be trained first. To do so, we create a training dataset consisting

Please verify that (1) all pages are present, (2) all figures are correct, (3) all fonts and special characters are correct, and (4) all text and figures fit within the red margin lines shown on this review document. Complete formatting information is available at http://SPIE.org/manuscripts

Return to the Manage Active Submissions page at http://spie.org/submissions/tasks.aspx and approve or disapprove this submission. Your manuscript will not be published without this approval. Please contact authorhelp@spie.org with any questions or concerns.

of 16 animals, encompassing a range of lesion sizes from small to large, along with their corresponding manual lesion masks. With no batch normalization and a Dice loss function optimized using Adam, the learning stops automatically with the early stopping criterion on the validation dice. According to the specificities of our project (stroke on the right hemisphere involving a brain deformation), we only use random crops of 128×128 pixels as data augmentation.

After the segmentation step, the 3D binary masks are cleaned to remove small regions located outside the lesion mask and to fill holes present inside the lesion mask. Our post-processing involves a median filter of size $[3, 3, 1]$ and a morphological opening filter of size $[5, 5, 1]$. Finally, only the largest connected component is retained. From DWI and T2H24 volumes we obtained the segmentations DWI_S and $T2H24_S$ which correspond respectively to the cytotoxic and vasogenic edema.

The T2H24 volume presents global edema (brain swelling on the ipsilateral side), causing misalignment with the other three volumes. It is necessary to register the T2H24 volume onto T2H0. This registration process involves employing both an Euler transform and a B-spline transform. Subsequently, the lesion mask segmented on T2H24 is propagated into the newly registered space as suggested in.[19]

3.3 Regions of Interest Computation

After the segmentation process, the three lesion masks $T2H24_S$, DWI_S and PWI_S are overlaid to extract the four regions of interest defined in.[2] Using our notations, these regions are obtained as follows (with $\overline{X_S}$ the binary complement of X_S):

$$\begin{aligned}
\text{Infarcted Ischemic Core: } & R_{IIC} = DWI_S \cap PWI_S \cap T2H24_S \\
\text{Salvaged Ischemic Core: } & R_{SIC} = DWI_S \cap PWI_S \cap \overline{T2H24_S} \\
\text{Salvaged Penumbra: } & R_{SP} = \overline{DWI_S} \cap PWI_S \cap \overline{T2H24_S} \\
\text{Infarcted Penumbra: } & R_{NSP} = \overline{DWI_S} \cap PWI_S \cap T2H24_S
\end{aligned}$$

4. RESULTS

Figure 2 gives an example of PWI segmentation based on two thresholds (0.75 and 0.62). For many slices, the overlap between manual and threshold segmentation is visually satisfactory. This also illustrates that PWI segmentation is not too threshold-sensitive.

An UNet segmentation results on a test rat, for both DWI and T2H24 MRI, is given in figure 3. For both MRI maps, automatic segmentation correctly locates and segments the ischemic zone. Even based on 2D UNet, the 3D consistency of the segmentations appears satisfactory.

We also evaluate quantitatively the segmentation. For $T2H24_S$ and DWI_S, Sørensen–Dice coefficient (Dice), Hausdorff Distance (HD, in mm), Average Symmetric Surface Distance (ASSD, in mm), and volume similarity[20] metrics are computed on 42 (for T2H24) and 44 (for DWI) animals 3D segmentation to compare the machine learning segmentation with the manual segmentation conducted by an expert. For PWI_S segmentation assessment, 60 animals are used for the assessment using the same metrics (because it does not need 16 for training). Table 1 summarizes the averaged metrics.

Additionally, a correlation curve is calculated to compare the volume computed by our automatic pipeline, with the manual segmentation for each sequence. These curves are shown in figure 4.

For all sequences, averaged Dice coefficients (for which values close to 1 mean close to the ground truth) are greater than 0.8. According to other metrics, and thanks to the post-processing, HD and ASSD errors are small and thus allow the volume similarity to be considered for further analysis as the ground truth and automatic prediction overlap in a large area. The volume similarities are also quite close to 0 which indicates very similar volumes between the two types of segmentation.

When analyzing volume correlation, figure 4 reveals very good performances of our approach for T2H24 and DWI with respectively $y = 0.889x$ ($R^2 = 0.996$) and $y = 0.848x$ ($R^2 = 0.996$) for a large range of lesion size. With $y = 0.965x$ ($R^2 = 0.987$), PWI automatic volumes segmentation is very correlated (in average) to manual segmentation but with a larger scattering of differences.

Please verify that (1) all pages are present, (2) all figures are correct, (3) all fonts and special characters are correct, and (4) all text and figures fit within the red margin lines shown on this review document. Complete formatting information is available at http://SPIE.org/manuscripts

Return to the Manage Active Submissions page at http://spie.org/submissions/tasks.aspx and approve or disapprove this submission. Your manuscript will not be published without this approval. Please contact authorhelp@spie.org with any questions or concerns.

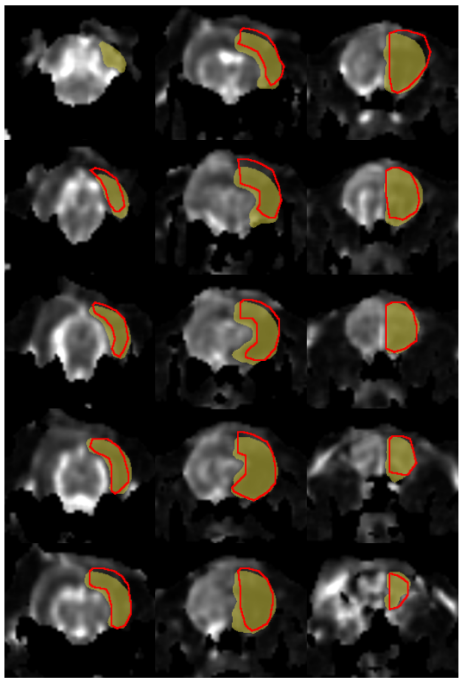

Figure 2: Example of PWI segmentation by optimized threshold. Each slice is displayed. The yellow area is manual segmentation, the green contour represents the segmentation with a threshold equal to 0.75, and the red contour represents segmentation with a threshold equal to 0.62.

Table 1: Segmentation quality assessment based on 4 metrics. 44 animals are averaged for DWI, 42 for T2H24 and 60 for PWI.

Metric	**DWI** mean ±std	**PWI** mean ±std	**T2H24** mean ±std
Dice	0.81 ±0.15	0.82 ±0.04	0.85 ±0.1
HD (mm)	2.16 ±1.22	1.99 ±1.04	2.28 ±0.74
ASSD (mm)	0.22 ±0.89	0.10 ±0.128	0.09 ±0.010
Volume Similarity	0.18 ±0.090	0.10 ±0.126	0.17 ±0.194

5. CONCLUSION

The deep learning segmentation demonstrates remarkable robustness in both T2H24 and DWI segmentation. The thresholding segmentation tends to perform less well, showing room for improvement. This might be due to the heterogeneity of perfusion data which makes them difficult to segment manually. As a consequence, the manual "ground truth" may not be very reliable. One limitation of our approach is the fact that we have used a semi-quantitative perfusion parameter, namely MPC. This is because partial volume effects hamper the definition of a proper arterial input function, devoid of partial volume effects. Hence deconvolution leading to quantitative parameters was not performed and Tmax maps (the clinical imaging biomarker of perfusion) were not available. We did not use time-to-peak maps because of the relatively low temporal resolution (one image per minute) due to technical limitations of our system.

In the future, improving acquisition and post-processing techniques will help us reproduce the same analysis as in the clinical setting for perfusion imaging. For now, to counteract this issue, we have incorporated a slider into the interface, allowing manual adjustment of the threshold value. Another limitation is the fact that we have tested the pipeline in one set of consecutive rats only, from a single scanner. It will be necessary to validate the approach using other independent sets of data. In conclusion, the proposed pipeline provides automatic

Please verify that (1) all pages are present, (2) all figures are correct, (3) all fonts and special characters are correct, and (4) all text and figures fit within the red margin lines shown on this review document. Complete formatting information is available at http://SPIE.org/manuscripts

Return to the Manage Active Submissions page at http://spie.org/submissions/tasks.aspx and approve or disapprove this submission. Your manuscript will not be published without this approval. Please contact authorhelp@spie.org with any questions or concerns.

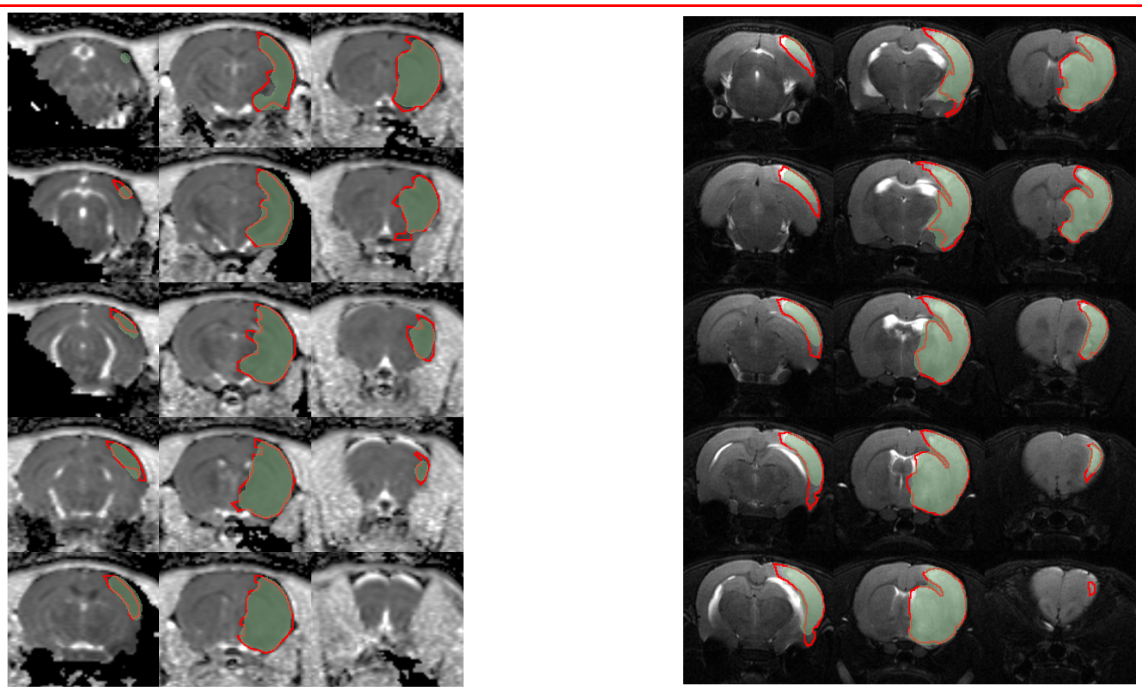

(a) UNet DWI (b) UNet T2H24

Figure 3: Example of a test rat segmented with UNet (left: DWI, right: T2H24). Each slice is displayed. The red outline represents manual segmentation, while green area represents automatic segmentation.

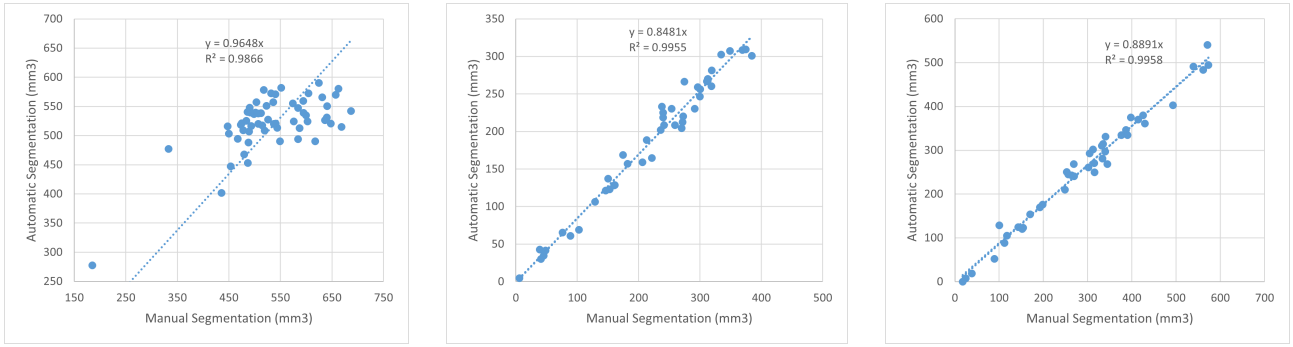

(a) PWI (b) DWI (c) T2H24

Figure 4: Correlation curves of volume similarity for the 3 segmented volumes against manual lesion size.

segmentation of multiparametric MRI data that may replace manual segmentation and thus increase both the efficiency and robustness of experimental stroke studies analysis.

ACKNOWLEDGMENTS

The research project has received funding by the French National Research Agency (ANR) grant BREAKTHRU (ANR18-CE19-0003).

This work was performed within the framework of the LABEX PRIMES (ANR-11-LABX-0063) of Université de Lyon, within the program "Investissements d'Avenir" (ANR-11-IDEX-0007) operated by the French National Research Agency (ANR).

SPIE USE: ____ DB Check, ____ Prod Check, Notes:

Please verify that (1) all pages are present, (2) all figures are correct, (3) all fonts and special characters are correct, and (4) all text and figures fit within the red margin lines shown on this review document. Complete formatting information is available at http://SPIE.org/manuscripts

Return to the Manage Active Submissions page at http://spie.org/submissions/tasks.aspx and approve or disapprove this submission. Your manuscript will not be published without this approval. Please contact authorhelp@spie.org with any questions or concerns.

REFERENCES

[1] Basalay, M. V., Wiart, M., Chauveau, F., Dumot, C., Leon, C., Amaz, C., Bolbos, R., Cash, D., Kim, E., Mechtouff, L., Cho, T.-H., Nighoghossian, N., Davidson, S. M., Ovize, M., and Yellon, D. M., "Neuroprotection by remote ischemic conditioning in the setting of acute ischemic stroke: a preclinical two-centre study," **10**(1), 16874 (2020).

[2] Debatisse, J. et al., "A non-human primate model of stroke reproducing endovascular thrombectomy and allowing long-term imaging and neurological read-outs," *Journal of Cerebral Blood Flow & Metabolism* **41**(4), 745–760 (2021). PMID: 32428423.

[3] E, C. and others/, "Multi-site laser doppler flowmetry for assessing collateral flow in experimental ischemic stroke: Validation of outcome prediction with acute MRI," **37**(6) (2017). Publisher: J Cereb Blood Flow Metab.

[4] Leclerc, S., Smistad, E., Pedrosa, J., Østvik, A., Cervenansky, F., Espinosa, F., Espeland, T., Berg, E. A. R., Jodoin, P.-M., Grenier, T., Lartizien, C., D'hooge, J., Lovstakken, L., and Bernard, O., "Deep learning for segmentation using an open large-scale dataset in 2d echocardiography," *IEEE Transactions on Medical Imaging* **38**, 2198–2210 (Sep. 2019).

[5] Wargnier-Dauchelle, V., Grenier, T., Durand-Dubief, F., Cotton, F., and Sdika, M., "A weakly supervised gradient attribution constraint for interpretable classification and anomaly detection," *IEEE Transactions on Medical Imaging* , 1–1 (2023).

[6] Chen, E., Barile, B., Durand-Dubief, F., Grenier, T., and Sappey-Marinier, D., "Multiple sclerosis clinical forms classification with graph convolutional networks based on brain morphological connectivity," *Frontiers in Neuroscience* **17** (2024).

[7] Dumortier, L., Guépin, F., Delignette-Muller, M. L., Boulocher, C. B., and Grenier, T., "Deep learning in veterinary medicine, an approach based on cnn to detect pulmonary abnormalities from lateral thoracic radiographs in cats," *Scientific Reports* **12** (2022).

[8] Nguyen, H.-T., Croisille, P., Viallon, M., Leclerc, S., Grange, S., Grange, R., Bernard, O., and Grenier, T., "Robustly segmenting quadriceps muscles of ultra-endurance athletes with weakly supervised u-net," in [*International Conference on Medical Imaging with Deep Learning – Extended Abstract Track*], (July 2019).

[9] Ronneberger, O., Fischer, P., and Brox, T., "U-net: Convolutional networks for biomedical image segmentation," in [*Medical Image Computing and Computer-Assisted Intervention – MICCAI 2015*], 234–241, Springer International Publishing, Cham (2015).

[10] Cai, L., Gao, J., and Zhao, D., "A review of the application of deep learning in medical image classification and segmentation," *Annals of Translational Medicine* **8**(11) (2020).

[11] Siddique, N., Paheding, S., Elkin, C. P., and Devabhaktuni, V., "U-net and its variants for medical image segmentation: A review of theory and applications," *IEEE Access* **9**, 82031–82057 (2021).

[12] Isensee, F., Jaeger, P. F., Kohl, S. A. A., Petersen, J., and Maier-Hein, K. H., "nnu-net: Self-adapting framework for u-net-based medical image segmentation," *Nature Methods* **18**, 203–211 (2021).

[13] Hatamizadeh, A., Tang, Y., Nath, V., Yang, D., Myronenko, A., Landman, B., Roth, H. R., and Xu, D., "Unetr: Transformers for 3d medical image segmentation," in [*2022 IEEE/CVF Winter Conference on Applications of Computer Vision (WACV)*], 1748–1758 (2022).

[14] Lee, H. H., Gu, Y., Zhao, T., Xu, Y., Yang, J., Usuyama, N., Wong, C., Wei, M., Landman, B. A., Huo, Y., et al., "Foundation models for biomedical image segmentation: A survey," *arXiv preprint arXiv:2401.07654* (2024).

[15] Khmelinskii, A. et al., "A visualization platform for high-throughput, follow-up, co-registered multi-contrast MRI rat brain data," in [*Medical Imaging 2013: Biomedical Applications in Molecular, Structural, and Functional Imaging*], **8672**, 439–445, SPIE (2013).

[16] Klein, S. et al., "elastix: A toolbox for intensity-based medical image registration," *IEEE Transactions on Medical Imaging* **29**(1), 196–205 (2010).

[17] Shamonin, D. P. et al., "Fast parallel image registration on cpu and gpu for diagnostic classification of alzheimer's disease," *Frontiers in Neuroinformatics* **7**, 1–15 (January 2014).

[18] Cardoso, M. J. et al., "MONAI: An open-source framework for deep learning in healthcare," (2022).

Please verify that (1) all pages are present, (2) all figures are correct, (3) all fonts and special characters are correct, and (4) all text and figures fit within the red margin lines shown on this review document. Complete formatting information is available at http://SPIE.org/manuscripts

Return to the Manage Active Submissions page at http://spie.org/submissions/tasks.aspx and approve or disapprove this submission. Your manuscript will not be published without this approval. Please contact authorhelp@spie.org with any questions or concerns.

[19] Koch, S. et al., "Atlas registration for edema-corrected mri lesion volume in mouse stroke models," *Journal of Cerebral Blood Flow & Metabolism* **39**(2), 313–323 (2019). PMID: 28829217.

[20] Reinke, A. et al., "Common limitations of image processing metrics: A picture story," (2022).

SPIE USE: ____ DB Check, ____ Prod Check, Notes: